Inorganic Chemistry

ARTICLE

pubs.acs.org/IC

Bidirectional "Ping-Pong" Energy Transfer and 3000-Fold Lifetime Enhancement in a Re(I) Charge Transfer Complex

James E. Yarnell, Joseph C. Deaton, Catherine E. McCusker, and Felix N. Castellano*

Department of Chemistry and Center for Photochemical Sciences, Bowling Green State University, Bowling Green, Ohio 43403, United States

Supporting Information

ABSTRACT: The synthesis and photophysics of a new Re(I)-carbonyl diimine complex, Re(PNI-phen)$(CO)_3$Cl, where the PNI-phen is *N*-(1,10-phenanthroline)-4-(1-piperidinyl)naphthalene-1, 8-dicarboximide is reported. The metal-to-ligand charge transfer (MLCT) emission lifetime was increased approximately 3000-fold at room temperature with respect to that of the model complex [Re(phen)$(CO)_3$Cl] as a result of thermal equilibrium between the emissive ^{3}MLCT state and a long-lived triplet ligand-centered (^{3}LC) state on the PNI chromophore. This represents the longest excited state lifetime (τ = 651 μs) that has ever been observed for a Re(I)-based CT photoluminescence at room temperature. The energy transfer processes and the associated rate constants leading to the establishment of the excited state equilibrium were elucidated by a powerful combination of three techniques (transient visible and infrared (IR) absorption and photoluminescence), each applied from ultrafast to the micro/milliseconds time scale. The MLCT excited state was monitored by transient IR using CO vibrations through time intervals where the corresponding signals obtained in conventional visible transient absorption were completely obscured by overlap with strong transients originating from the pendant PNI chromophore. Following initial excitation of the ^{1}LC state on the PNI chromophore, energy is transferred to form the MLCT state with a time constant of 45 ps, a value confirmed in all three measurement domains within experimental error. Although transient spectroscopy confirms the production of the ^{3}MLCT state on ultrafast time scales, Förster resonance energy transfer calculations using the spectral properties of the two chromophores support initial singlet transfer from ^{1}PNI* to produce the ^{1}MLCT state by the agreement with the experimentally observed energy transfer time constant and efficiency. Intersystem crossing from the ^{1}MLCT to the ^{3}MLCT excited state is believed to be extremely fast and was not resolved with the current experiments. Finally, triplet energy was transferred from the ^{3}MLCT to the PNI-centered ^{3}LC state in less than 15 ns, ultimately achieving equilibrium between the two excited states. Subsequent relaxation to the ground state occurred via emission resulting from thermal population of the ^{3}MLCT state with a resultant lifetime of 651 μs. The title chromophore represents an interesting example of "ping-pong" energy transfer wherein photon excitation first migrates away from the initially prepared ^{1}PNI* excited state and then ultimately returns to this moiety as a long-lived excited triplet which disposes of its energy by equilibrating with the photoluminescent Re(I) MLCT excited state.

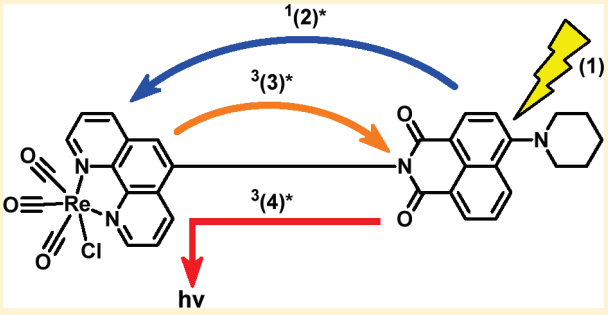

INTRODUCTION

The absorption, photophysical, and redox properties of d^6 transition metals continue to receive considerable attention, including those based on Re(I).[1] Rhenium(I) carbonyl-diimine (Re-CDI) complexes are photo- and redox active complexes that can be incorporated into supramolecular systems, polymers, and biomolecules because of their chemical robustness and synthetic flexibility.[2] With this adaptability, Re-CDI complexes can be used in a multitude of applications including solar energy conversion,[3,4] luminescence sensing,[5−14] biotechnology,[15,16] photochemical molecular devices,[17,18] and solar fuels photochemistry.[19−23]

In many Re-CDI complexes, photoluminescence originates from a lowest energy triplet excited state displaying metal-to-ligand charge transfer (MLCT) character.[24−26] It is possible that other states such as ligand-centered (LC) triplet states could emit independently of this MLCT emission if these states do not readily interconvert.[27] However, if the states interconvert on a sufficiently fast time scale, a thermal equilibrium will be established between them, and the emission properties can be described as a Boltzmann average. In particular, the excited state lifetime will greatly exceed what is normally observed for MLCT emission to the extent that the equilibrium is tipped toward a ^{3}LC state having a very long lifetime.[28] Numerous examples of molecular systems having two excited states in thermal equilibrium include complexes of metals containing Ru,[29−39] Pt,[40,41] Os,[42,43] Ir,[44] Cu,[45,46] and W,[47] many of which have been recently reviewed.[48] Contributions from our laboratory have included investigations of Ru(II) MLCT complexes covalently linked to pyrene or naphthalimide chromophores.[34−37] For example, in

Received: May 9, 2011
Published: July 15, 2011

Scheme 1. Series of Reactions Required to Produce Re(PNI-phen)$(CO)_3$Cl (1)

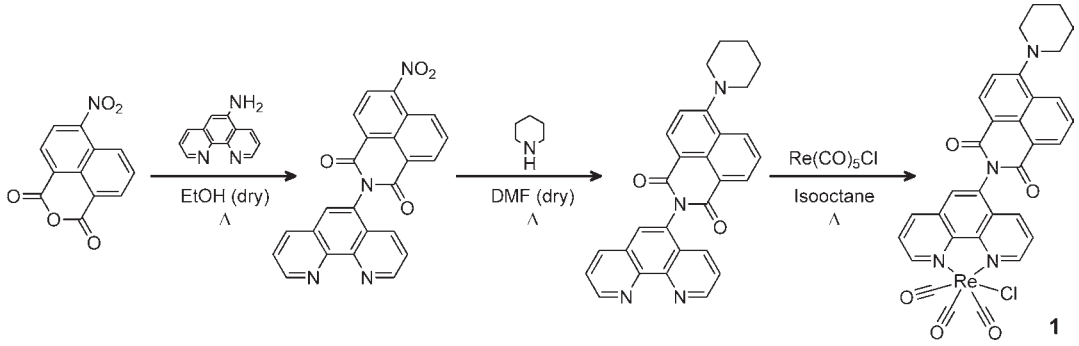

select molecules, the lifetime of emission observed at room temperature was extended from less than 1 μs for the model complex, $[Ru(bpy)_3]^{2+}$, to around 3 and 40 μs with attachment of a single pyrene or napthalimide chromophore, respectively.[34,36] It is important to note that the precise number of appended ^{3}LC-bearing moieties in equilibrium with the triplet emitting state offer systematic excited state lifetime tuning[34−38,48] otherwise not possible using more conventional nonradiative decay-reducing approaches such as the energy gap law,[49,50] delocalization phenomena,[51,52] or ligand strain relief.[53] Very recently, the excited state equilibrium concept has been applied to new classes of molecular structures, including those based on a ZnTPP-tungsten alkylidyne,[47] and BODIPY-Benzoporphyrin.[41] Such molecules are of fundamental importance toward understanding singlet−triplet partitioning and exciton management required for the optimization of next generation device technologies including organic light emitting diodes,[46,54−56] organic photovoltaics,[41,57] and photochemical upconversion.[58] In our opinion, continuing investigations of relatively complex photophysical molecular phenomena will generate fundamental knowledge poised for integration into desired applications.

One objective of the present study was to achieve an excited state lifetime in a Re-CDI complex suitable for supporting high efficiency diffusion-based chemistry while simultaneously increasing its visible absorption cross-section by attaching an organic chromophore with strong $\pi-\pi^*$ ^{1}LC absorptions overlapping the lower energy portion of the Re→phen ^{1}MLCT bands. A 3000-fold increase in excited state lifetime was achieved in the present work by covalently attaching a 4-piperidinyl-1,8-naphthalimide (PNI) chromophore to the 5-position of 1,10-phenanthroline (PNI-phen) and preparing a new Re(I) complex, Re(PNI-phen)$(CO)_3$Cl (**1**). While similar Re-CDI complexes exist,[59] the lifetime increase in the present case is by far the largest.

An equally important objective of the current study is to elucidate the energy transfer processes leading to excited state equilibrium and their associated kinetics. In prior studies on PNI-phen complexes of Ru(II), we were able to monitor the ligand-centered excited state using both transient absorption (TA)[36] and time-resolved infrared (TRIR) spectroscopy[60] on the nanosecond time scale. In the present study of the Re(I) complex, we extend both of these techniques to the femtosecond time domain to observe the early time evolution of intermediates leading to the population of the ^{3}LC state of the PNI subunit. We also succeeded in observing the Förster-type fluorescence quenching of the initially populated ^{1}LC state using time-correlated single photon counting (TCSPC). While the ^{3}MLCT signals in TA were largely obscured on most time scales resulting from overlap with signals from the PNI chromophore, the C≡O stretching vibrations of the Re(I) complex provided a critical spectroscopic handle that enabled ^{3}MLCT excited state evolution to be monitored by TRIR techniques on both fs and ns time scales.

RESULTS AND DISCUSSION

Synthesis. The PNI-phen ligand[36] and the Re(PNI-phen)-$(CO)_3$Cl (**1**) complex were synthesized as outlined in Scheme 1 with the final complex being purified with flash chromatography. ^{1}H NMR and mass spectra of the PNI-phen ligand and its respective precursors are comparable to those published previously.[36] The structure of title compound **1** was confirmed by ^{1}H, ^{13}C, and ^{1}H-^{1}H COSY NMR spectra, MALDI-TOF MS, and FT-IR spectroscopy. This complex is both thermally and photochemically stable in both the solid state and solution, being soluble in a variety of organic solvents. In the present study, tetrahydrofuran (THF) was selected because of its favorable spectroscopic window in the mid-IR enabling direct time-resolved vibrational visualization of the carbonyl and carbon monoxide subunits resident on the PNI chromophore and the Re(I) metal center, respectively.

Absorption and Photoluminescence Spectroscopy. In the present study, the model used for the PNI chromophore was *N*-(4-methylphenyl)-4-(1-piperidinyl)naphthalene-1,8-dicarboximide (PNI).[36] This model was found to have nearly identical photophysical properties to the free ligand PNI-phen reported in a prior study.[36] The low energy portion of the absorption spectra of Re(phen)$(CO)_3$Cl, **1**, and PNI in THF are presented in Figure 1. This spectral region is purposely emphasized as only low energy excitation processes are relevant to the processes described in this manuscript. The main absorption band of the parent Re(phen)$(CO)_3$Cl complex (λ_{max} = 386 nm) has been previously assigned as ^{1}MLCT in nature.[61] The lowest energy absorption of the PNI chromophore has also been assigned as a ^{1}CT transition.[36,62−65] The absorption spectrum of **1** is approximately the sum of that of the two constituent model chromophores, Re(phen)$(CO)_3$Cl and PNI, with the exception of being red-shifted by approximately 10 nm (data not shown). The absorption spectra of the model constituent chromophores substantially overlap so selective excitation of either within **1** cannot be readily achieved.

The emission spectrum of a deaerated solution of **1** at room temperature (RT) is compared to that obtained after the sample was exposed to air, Figure 2a. The deaerated solution exhibited two emission bands, and only the one at longer wavelength was

dx.doi.org/10.1021/ic200974h |*Inorg. Chem.* 2011, 50, 7820–7830

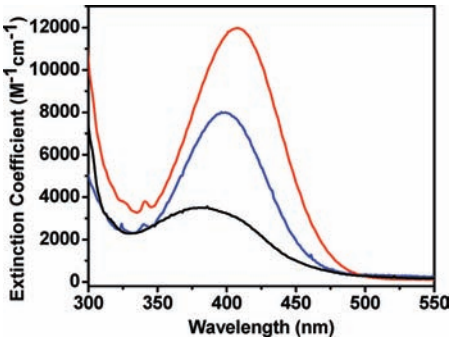

Figure 1. Static electronic spectra of Re(phen)$(CO)_3$Cl (**black**), **1** (**red**), and PNI (**blue**) in THF at RT.

quenched upon exposure to air, demonstrating that the latter likely arises from a triplet state and the one at shorter wavelengths originates from a singlet state. The phosphorescence of **1** was obtained by subtracting the spectrum of the sample after exposure to air from that of the deaerated sample and is compared in Figure 2b to the emission of the MLCT model complex Re(phen)$(CO)_3$Cl. The two spectra are nearly identical in λ_{max} and band shape. The excitation spectrum (not shown) of emission monitored at the long wavelength peak maximum matched the absorption spectrum.

The singlet emission of the oxygen-quenched complex has very similar wavelength and band shape with respect to that of the free PNI model compound, but is nearly quantitatively quenched relative to the free PNI, as indicated in Figure 2c. The quenching of the singlet fluorescence of the PNI moiety in the bichromophore is also reflected in the lifetime of its fluorescence emission. From measurements made by TCSPC, the excited state lifetime (τ) for the PNI emission measured at 509 nm decreases from 7.64 ns in the free PNI model to 49 ps in **1** (Table 1). The corresponding energy transfer rate, k_{et}, is therefore 2.04×10^{10} s^{-1}, and these lifetime data yield an energy transfer efficiency of 99.4%. Even though the fluorescence spectrum of the free PNI is red-shifted relative to the main ^{1}MLCT absorption of the model Re(phen)$(CO)_3$Cl (Supporting Information, Figure S1), there remains some significant spectral overlap enabling Förster-type energy transfer from the PNI chromophore to the Re(I) MLCT complex. Förster energy transfer parameters were determined using PhotochemCAD in conjunction with these spectral data and a 9.5 Å chromophore separation distance, roughly the distance between the metal center and PNI from previous molecular modeling.[36,66−68] These calculations predict a k_{et} value of 1.26×10^{10} s^{-1} and a corresponding energy transfer efficiency of 99.0%, with $J = 5.20 \times 10^{-16}$ M^{-1} cm^3 and a Förster distance of 20.4 Å. Both former values are in good agreement with those determined experimentally.

The photoluminescence emission intensity decay of a deaerated THF solution containing **1** was adequately fit to a single exponential function (Supporting Information, Figure S2). The emission spectrum was independent of concentration, but the intensity decays displayed concentration-dependent dynamic quenching (Figure 3). The latter has been previously observed in the related long-lifetime Ru(II)-PNI-containing polychromophores,[36] so it is not surprising that a similar phenomenon is observed here, particularly with such a remarkably extended excited state lifetime. Through concentration-dependent dynamic Stern−Volmer analysis,[69] the self-quenching rate constant

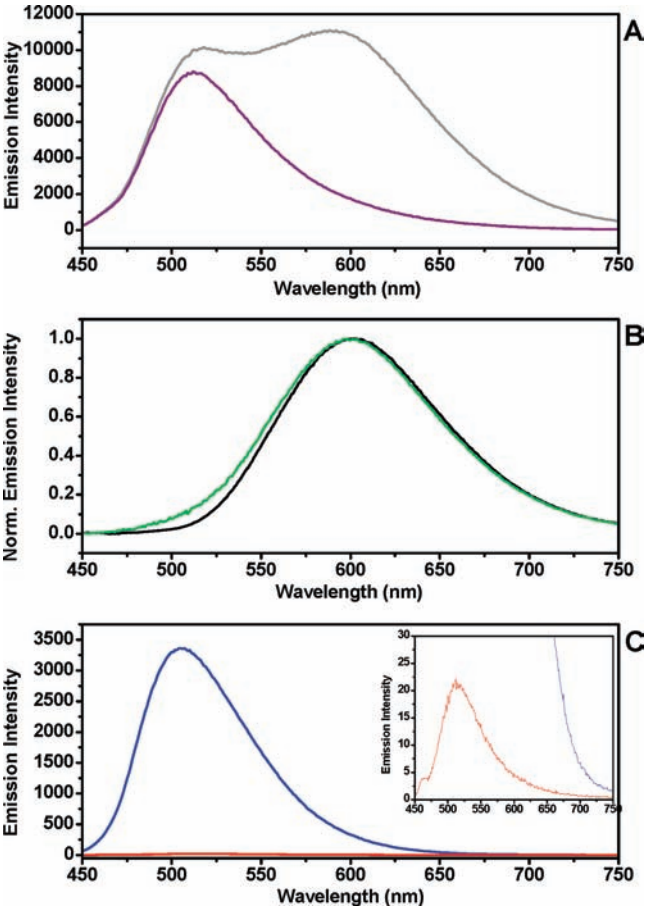

Figure 2. (a) Static emission spectra of deaerated (**gray**) and aerated solutions of 0.177 mM **1** (**purple**) in THF with 410 nm excitation. (b) Phosphorescence spectrum of **1** (**green**) obtained by subtracting the spectrum of the sample after exposure to air from that of the deaerated sample and the static emission spectrum of dearated Re(phen)$(CO)_3$Cl (**black**) in THF (410 nm excitation). (c) Static emission spectra of air-equilibrated, optically matched (0.1 O.D. at 410 nm) THF solutions of PNI (**blue**) and **1** (**red**) Inset: Expanded view of **1**′s photoluminescence using the same data presented in panel C.

was determined to be 2.14×10^8 M^{-1} s^{-1}. The quantum yield likewise displayed concentration-dependent quenching (Supporting Information, Figure S3). At theoretical infinite dilution, the emission quantum yield of **1** is remarkably close to that of the model complex Re(phen)$(CO)_3$Cl, but its triplet CT emission lifetime (τ = 651 μs) is approximately 3000-fold larger, Table 1. This immediately implies that the MLCT emission lifetime in **1** is being significantly perturbed by the pendant PNI subunit, and the likely origin of this effect is a thermal equilibrium between the two species at RT.[28,34,36,37,48]

In a frozen 2-methyl-THF (MTHF) glass at 77 K, the emission profile of the Re(phen)$(CO)_3$Cl model was strongly blue-shifted (Figure 4a), consistent with the polar nature of the CT excited state,[61] but a corresponding MLCT band was not readily apparent in the corresponding steady-state emission spectrum of **1**. Instead, the steady-state spectrum of **1** at 77 K was dominated by the residual singlet fluorescence of the PNI moiety, and a band at 600 nm containing a shoulder near 650 nm. The photoluminescence decay in the long wavelength region, excluding the residual PNI fluorescence, was biexponential, unlike the single exponential

Table 1. Photophysical Data of the Chromophores in This Study[a]

molecule	$\lambda_{abs\ max}$ (nm) (ε, $M^{-1}\ cm^{-1}$)	$\lambda_{em\ max}$ (nm) (298 K)	τ_{em} (298 K)[b]	$\lambda_{em\ max}$ (nm) (77 K)	τ_{em} (77 K)[b]	Φ_{em}[c]
[Re(PNI-phen)$(CO)_3$Cl]	408 (11980)	509, 593	49 ps,[d] 651 μs[e]	493,[f] 595[f] 530,[g] 600[h]	5.8 μs,[i] 270 ms[j]	0.013[e]
[Re(phen)$(CO)_3$Cl]	386 (3550)	594	197 ns	524	7.6 μs[k]	0.013[k]
PNI	396 (8005)	504	7.64 ns	482		0.93

[a] Room temperature measurements were made with THF as a solvent while 77 K measurements were made with 2-methyl-THF. All solutions were degassed except as noted. [b] Emission decay measurements were performed using a nitrogen pumped dye laser apparatus with the exception of PNI and the air-saturated **1** (residual fluorescence) which were measured using TCSPC. The excitation wavelength for all measurements was set to 410 nm, and the emission was collected at 650 nm for **1**, 600 nm for Re(phen)$(CO)_3$Cl, and 505 nm for PNI at room temperature. Emission was collected at 600 nm for **1** and for Re(phen)$(CO)_3$Cl at 77 K. [c] Quantum yields were measured using $[Ru(bpy)_3]Cl_2$ as the standard.[24,34] [d] Fast component (residual fluorescence) measured for air-saturated **1**. [e] The photoluminescence lifetime and the quantum yield of deaerated **1** at room temperature were determined in the absence of self-quenching (theoretical infinite dilution) from the concentration dependence. [f] Steady-state emission maxima. [g] Time-resolved emission maximum after 5 μs delay. [h] Time-resolved emission maximum after 25 ms delay. [i] Photoluminescence decay of the short component (excluding residual PNI fluorescence) measured at 540 nm. [j] Photoluminescence decay of the long component measured at 650 nm. [k] Values are referenced from ref 70.

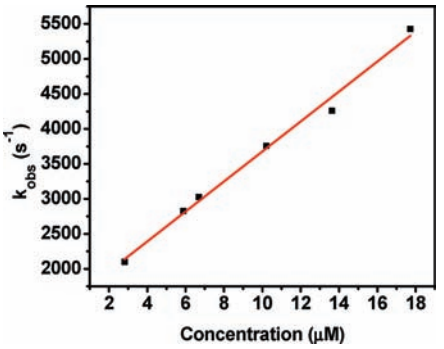

Figure 3. Self-quenching of **1** measured in deaerated THF at 22 °C using the N_2-pumped broadband dye laser system (410 nm excitation, 500 ps fwhm). Sample was deaerated using the freeze−pump−thaw method.[71].

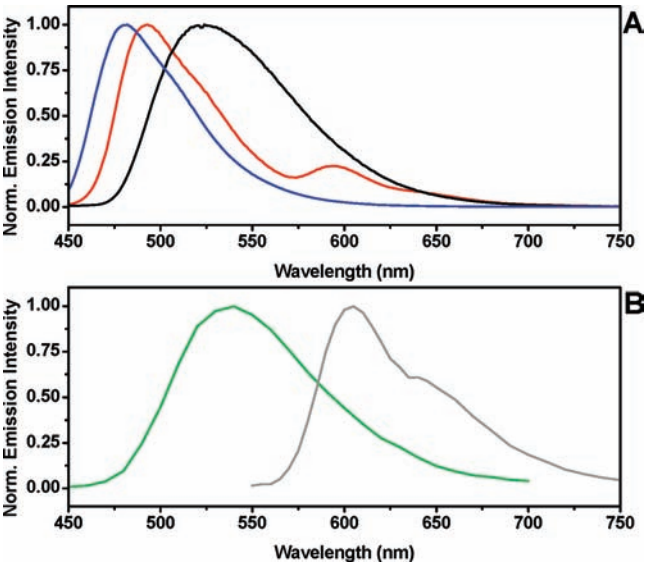

Figure 4. (a) Static 77 K emission spectra of Re(phen)$(CO)_3$Cl (**black**), **1** (**red**), and PNI (**blue**) in MTHF with 410 nm excitation. (b) Time-resolved 77 K emission spectra of **1** at 5 μs (**green**) and 25 ms (**gray**) after a 500 ps 410 nm laser pulse in MTHF.

decay observed in solution at 298 K. Consistent with the biexponential decay, time-resolved emission spectra at 77 K revealed two peaks (Figure 4b). The one revealed after a 5 μs delay has λ_{max} = 530 nm and closely resembles the 77 K emission spectrum of the Re(phen)$(CO)_3$Cl model. It had been obscured by the overlapping PNI band in the steady-state spectrum. The band recorded after 25 ms delay has λ_{max} = 600 nm and closely matches the phosphorescence spectrum previously assigned to the PNI moiety in a Ru-containing bichromophore.[36] Excluding the PNI fluorescence, the shorter lifetime component of the 77 K photoluminescence was more pronounced at the shorter wavelengths, and the longer component was larger at longer wavelengths, consistent with the time-resolved spectra. The decay time of the short component was determined to be 5.8 μs, very close to that of the Re(I) model complex under the same conditions (Table 1). The long lifetime component of the photoluminescence possesses a decay time of 270 ms, clearly indicating an organic chromophore lacking significant heavy-atom spin−orbit coupling, consistent with that expected for the ^{3}LC state of the PNI moiety.

The biexponential photoluminescence decay and time-resolved emission spectra clearly demonstrate that the ^{3}MLCT and ^{3}LC states do not readily interconvert at low temperature in the rigid glass. However, at RT in THF solution, **1** (excluding the weak residual fluorescence at shorter wavelengths) possesses a lifetime intermediate between those of the pure ^{3}MLCT and the pure ^{3}LC model chromophores. The latter is indeed indicative of thermal equilibrium between those two triplet excited states.[28,34,36,37,48] The energy separation between the states at 77 K can be estimated from the time-resolved spectra. In the absence of a definitive determination of the (0,0) emission origins, an approximation may be made by taking the emission energy at the point on the high-energy side of the respective peaks where the intensity is 25% of the maximum, leading to a rough estimate of ΔE as 3090 cm^{-1}. However, this estimate applies to the frozen glass and does not quantitatively address the situation in solution at RT because the different states likely have different rigido-chromic and solvent reorganizational effects. A better estimate lies in estimating the energy of the room temperature ^{3}MLCT state provided in Figure 2b using the same procedure described above, less the energy of the ^{3}LC state as established from the time-resolved emission spectrum at 77 K (Figure 4b), leading to ΔE = 1570 cm^{-1}.

The energy separation between ^{3}MLCT and ^{3}LC states at room temperature may also be evaluated from the observed decay rate using eqs 1−3. Here, the value for k_{obs} at infinite dilution

(Table 1) was used to eliminate concentration quenching effects. For k_{MLCT}, the inverse lifetime for the Re(phen)$(CO)_3$Cl model is a good approximation since the photoluminescence spectra and the quantum yields at room temperature are quantitatively similar to **1**. We were unable to obtain a reliable value for k_{LC} at room temperature by triplet sensitization of free PNI in THF using thioxanthone because of strong concentration quenching and weak transient signals. Therefore, the value of k_{LC} determined above for the PNI chromophore in **1** at 77 K was used to approximate the rate constant. This assumption is not likely to introduce a large error even if k_{LC} is in fact greater at room temperature because the k_{MLCT} is 6 orders of magnitude greater than the 77 K value of k_{LC}. Using these estimates of k_{MLCT} and k_{LC}, ΔE = 1680 cm^{-1} which is in close agreement with the 1570 cm^{-1} value estimated above from the spectral data.

$$k_{obs} = \alpha[k_{LC}] + (1-\alpha)[k_{MLCT}] \quad (1)$$

$$K_{eq} = \frac{^3LC}{^3MLCT} = \frac{\alpha}{1-\alpha} \quad (2)$$

$$\Delta E = -RT\ln(K_{eq}) \quad (3)$$

Ultrafast Transient Absorption. Figure 5a displays the excited state absorption difference spectra for **1** measured on the ultrafast time scale. As reported by Greenfield and coworkers,[65] the ^{1}LC state of the PNI moiety is visualized by a strong excited state absorption centered at 445 nm and corresponding stimulated emission at 540 nm. Both the excited state absorbance and the stimulated emission decay with the same time constant of τ = 44 ps (Figure 5b and 5c), in excellent quantitative agreement with the decay of the residual PNI fluorescence measured by TCSPC, τ = 49 ps. After the ^{1}LC features had largely depopulated by 100 ps, a broad absorption band centered at 480 nm persisted for the duration of the experiment (1.5 ns). This particular excited state absorption feature has been quantitatively reproduced in the present model complex Re(phen)$(CO)_3$Cl on the same time scale under the identical experimental conditions and is clearly attributable to the ^{3}MLCT excited state (Supporting Information, Figure S4). We note that similar transient features have been observed in related Re(I)-CDIs.[70,72,73] The kinetics related to the production of the ^{3}MLCT state in **1** could not be tracked because of significant overlap with the ^{1}PNI* absorbance and its stimulated emission. Features that could potentially be ascribed to a ^{1}MLCT intermediate as implied by the Förster energy transfer studies were not observed for **1**, consistent with extremely rapid intersystem crossing typical of MLCT states.[74] In ultrafast transient absorption, the initial formation of ^{1}PNI* leads directly to the observation of the ^{3}MLCT* which persists to the end of the experimental time regime (1.5 ns).

Ultrafast TRIR Spectroscopy. The Re(PNI-phen)$(CO)_3$Cl complex possesses optimal IR markers useful for tracking both the MLCT and the ligand-centered excited states. On the Re(I) metal center in the ground state, the three metal C≡O bonds absorb very strongly at 2019, 1918, and 1893 cm^{-1}.[75] On the PNI ligand, the two C═O imide bonds absorb at 1714 and 1673 cm^{-1}.[60a] Figure 6 indicates a blue shift of the metal C≡O bonds immediately following 400 nm excitation, which is a direct result of reduced π-back-bonding in the MLCT excited state resulting from depletion of metal center electron density. The two C═O imide stretches display an opposite energy shift and

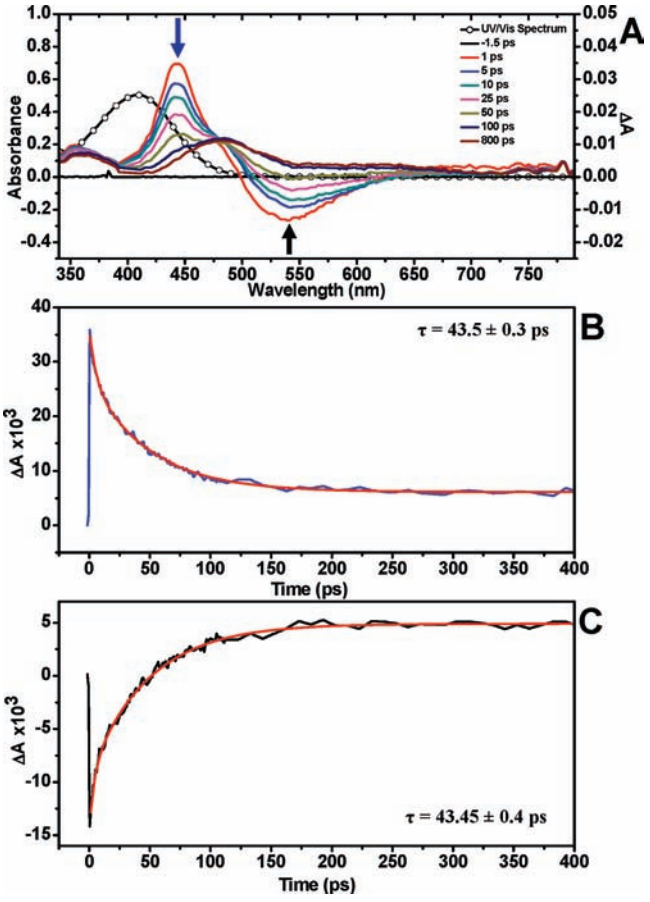

Figure 5. (a) Ground state UV/vis absorbance spectra and excited state absorption spectra of **1** in THF following 400 nm pulsed excitation (110 fs fwhm) with experimental delay times indicated. (b) Excited state transients of 445 nm (**blue**) of **1** in THF following 400 nm pulsed excitation (110 fs fwhm). (c) Excited state transients of 540 nm (**black**) of **1** in THF following 400 nm pulsed excitation (110 fs fwhm). The red lines in Figure 5a and 5b are the single time constant fits to the absorption transients.

direction of signal change with time. The infrared vibrational frequencies are collected in Supporting Information, Table S1. The absorptions of the imide stretches in the molecular excited state appear red-shifted relative to the two ground state C═O bleaching signals. The kinetics of these transients are presented in Figure 7, which compares the growth of the metal carbonyl stretch at 1945 cm^{-1} and the decay of the imide vibrational stretch at 1645 cm^{-1}. The observed time-constants for both these processes match what was observed by the femtosecond TA and TCSPC for the decay of the ^{1}LC state localized on PNI. Because the ground state ^{1}MLCT and ^{1}LC absorption bands overlap, a portion of the population of molecules is likely excited directly into the ^{1}MLCT state. This accounts for the nonzero ΔA for the C≡O stretch at t = 0 in the TRIR experiments (Figure 7, bottom).

Nanosecond Transient Absorption Spectroscopy. The formation of the ^{3}LC state can be clearly observed in the nanosecond TA experiment. Figure 8 shows two broad excited state bands centered at 470 and 680 nm, which are associated with the ^{3}LC state of the PNI moiety by comparison to results from our previous study.[36] The only ground state bleaching observed (~400 nm) is consistent with depletion of the ^{1}CT band of

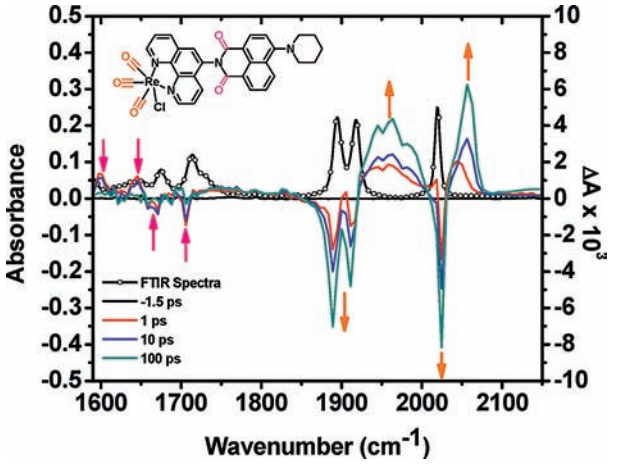

Figure 6. Ground state FT-IR spectrum and time-resolved infrared difference spectrum of **1** in THF following 400 nm pulsed excitation (90 fs fwhm). The spectral resolution for the time-resolved measurements was approximately 4 cm^{-1} and the experimental delay times are specified.

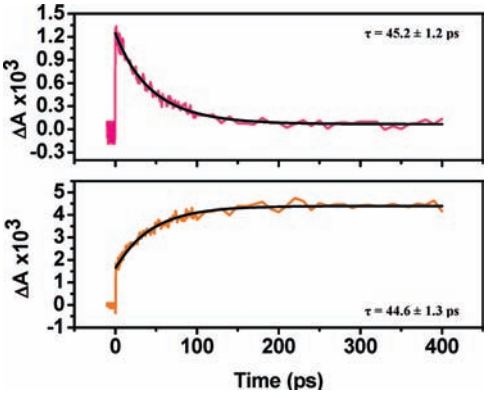

Figure 7. Single wavelength IR transients measured at 1645 cm^{-1} (**pink**) and 1945 cm^{-1} (**orange**) for **1** in THF following 400 nm pulsed excitation (110 fs fwhm).

the PNI moiety. The transient assigned to the ^{3}MLCT state that was present at the end of the 1.5 ns duration of the femtosecond TA experiment was not clearly resolved in the nanosecond TA because of substantial overlap with the ^{3}PNI* transients. The growth of the ^{3}PNI* state occurred promptly (τ < 15 ns) making it impossible to extract a precise time constant for its formation because of the time resolution of this instrument. The process taking place between 1.5−15 ns, the only missing time window in this study, is most likely triplet−triplet energy transfer between the ^{3}MLCT excited state and the ^{3}LC (^{3}PNI) states. The subsequent decay of the ^{3}LC excited state as ascertained by laser flash photolysis was found to be kinetically superimposable with the ^{3}MLCT photoluminescence decay of the identical sample (Figure 9), demonstrating that these two states are in rapid thermal equilibrium and decay to the ground state with the same time constant. This confirms the earlier conclusion drawn from the fact that the photoluminescence intensity decay was single exponential with a lifetime intermediate between those of the Re(I) model complex and the free PNI chromophore. Since the ^{3}LC state is lower in energy with respect to the ^{3}MLCT state and the RT lifetime strongly lies toward that of the ^{3}PNI* 77 K lifetime, the

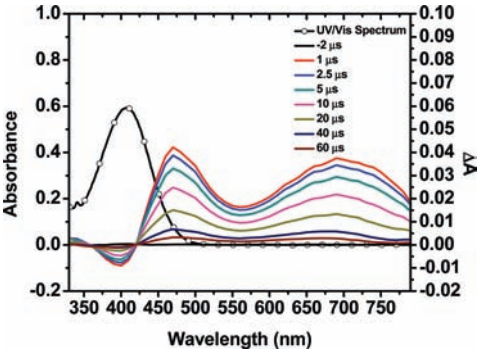

Figure 8. Ground state UV/vis absorbance spectra and excited state absorption difference spectra of **1** in THF following 410 nm pulsed excitation (5−7 ns fwhm). The sample was purged with high quality argon and pumped through a flow cell with a path length of 1 cm, and the experimental delay times are indicated.

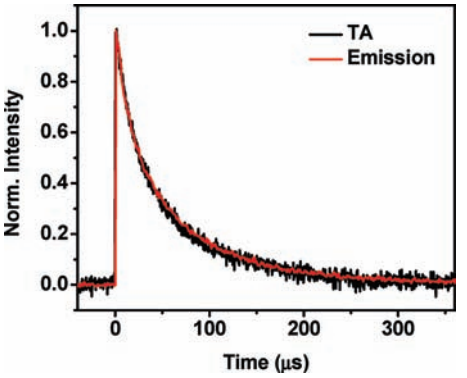

Figure 9. Comparison of 34 μM **1** sample measured in deaerated THF at 22 °C using the nanosecond TA transient feature at 470 nm (**black line**) and the photoluminescence transient measured at 600 nm (**red**). The sample was deaerated using the freeze−pump−thaw method.[71]

majority of the excited state clearly resides on the ^{3}LC state in **1**. This triplet state is long-lived because it is not well coupled to the metal center, producing excited state decay controlled by equilibrium population of the ^{3}MLCT state and not by spin−orbit coupling.

Nanosecond Step-Scan FTIR. The nanosecond step-scan FTIR spectra of **1** are presented in Figure 10, and the vibrational frequencies are listed in Supporting Information, Table S1. The ground state bleaches and excited state absorptions of the C≡O stretches associated with the MLCT excited state that were observed to grow with a time constant of 45 ps in the femtosecond TRIR (Figures 6 and 7) were found to decrease within about 60 ns in the step-scan experiment, Figure 10. By 60 ns after the 410 nm (5−7 ns fwhm) laser pulse, new C≡O excited state absorptions appeared that revealed slight red shifts relative to the ground state absorptions. This phenomenon has been reported in previous studies of metal carbonyl complexes containing ^{3}LC excited states.[76] This result clearly indicates that the excited state is no longer of ^{3}MLCT parentage as the C≡O transients no longer indicate its presence at longer delay times. At the same time, ground state bleaches and excited state absorptions corresponding to the C═O imide stretches were produced at nearly the same frequencies where decays were observed with a time constant of 45 ps in the ultrafast TRIR experiments (Figures 6 and 7; Supporting Information, Table S1). The 45 ps decay time

dx.doi.org/10.1021/ic200974h |*Inorg. Chem.* 2011, 50, 7820–7830

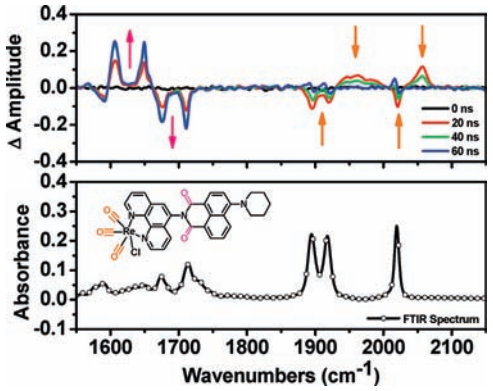

Figure 10. Ground-state FTIR spectra and time-resolved step-scan FTIR difference spectrum of **1** in THF following 410 nm pulsed excitation (5−7 ns fwhm). The sample was purged with high quality argon and pumped through a flow cell with a path length of 330 μm. The spectral resolution for the time-resolved measurements was approximately 8 cm^{-1}, and the approximate experimental delay times are indicated.

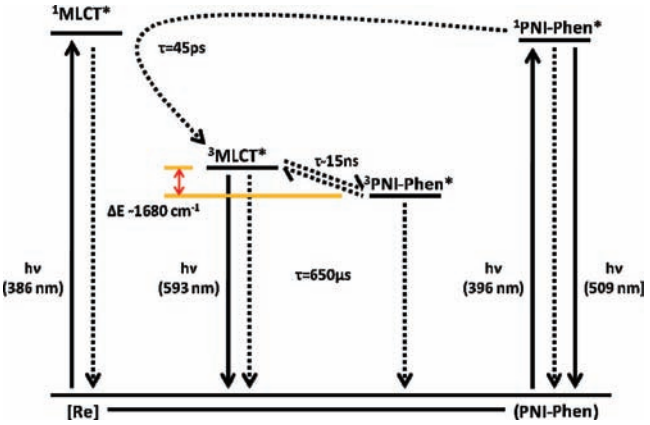

Figure 11. Energy level diagram describing the photophysical processes of **1** in THF at room temperature. The solid lines represent radiative transitions, and the dashed lines represent nonradiative transitions. The presented time constants (τ) are the inverse of the observed rate constants for the associated processes. See text for details.

constants associated with those IR transients were assigned to the decay of the ^{1}LC excited state of the PNI moiety, an assignment strongly supported by independent TCSPC and ultrafast TA experiments. The absorptions and bleaches generated on the nanosecond and longer time scales are consistent with the production of the ^{3}LC on PNI, precisely the same conclusion drawn from the nanosecond TA study. The imide vibrations of the ^{3}PNI* state have been previously examined in step-scan experiments on the PNI model and closely resemble the data presented in Figure 10.[60a] We also note that time-resolved IR spectroscopy has been performed on related Pt(II)-containing NDI structures and the associated ^{3}NDI LC excited state.[60b]

Excited State Evolution and Decay. The energy transfer, equilibrium, and decay processes occurring in the excited state of **1** are summarized in the energy level diagram displayed in Figure 11. The quenching of the initially prepared excited state identified as a PNI singlet was observed independently with TCSPC, fs TA, and fs TRIR to have a time constant of about 45 ps. The combined ultrafast measurements provided substantive spectroscopic evidence for the subsequent formation of the ^{3}MLCT excited state on the Re(I) complex. The kinetic formation of the ^{3}MLCT could not be clearly resolved with fs TA but was definitively assigned using fs TRIR with associated C≡O transient kinetics exhibiting an identical time constant to the ^{1}LC decay observed in the other two techniques. The formation of the ^{1}MLCT state as implied by resonance energy transfer sensitization experiments through the ^{1}PNI* moiety could not be resolved, presumably because of a combination of competitive absorption processes in concert with rapid intersystem crossing. Intersystem crossing is known to be very fast in related MLCT complexes, generally with time constants <200 fs.[74] The agreement between the observed quenching rate of the ^{1}LC state and energy transfer efficiency with respect to those values calculated using Förster theory strongly support the formation of the ^{1}MLCT state as an intermediate in the observed evolution from ^{1}LC to ^{3}MLCT parentage. The production of ^{3}PNI* was clearly resolved in both nanosecond TA and nanosecond IR as a prompt signal with a formation time constant <15 ns. Clear-cut transients related to ^{3}MLCT* could not be clearly resolved in flash photolysis experiments because of the sizable ^{3}PNI* transient signals. Although not reliable in terms of specific delay time, step-scan FTIR measurements display prompt difference spectra clearly attributable to ^{3}MLCT* that decay over the same time interval as transients related to ^{3}PNI* are produced, indicative of triplet energy transfer. The rather slow time constant, between 2 and 15 ns, for the triplet energy transfer is consistent with the PNI chromophore not being coupled to the MLCT chromophore, undoubtedly because the phen and the PNI are not conjugated because of rotation about the σ bond connecting them. Although the ^{3}MLCT had clearly decayed over the time of the ^{3}LC formation, photoluminescence continued to emerge from the ^{3}MLCT state in **1**. This photoluminescence intensity decay quantitatively matches the ^{3}PNI decay kinetics observed in the nanosecond TA experiment, ultimately illustrating that these two states are in rapid thermal equilibrium and that the emission emanates from the ^{3}MLCT state as a result of thermal activation. In contrast to the single exponential decay observed for the room temperature solutions (excluding the residual fluorescence of ^{1}LC), biexponential kinetics was necessary to adequately fit the luminescence intensity decays measured in MTHF at 77 K. The two emissions, now emerging as independent chromophores at low temperature and no longer arising from states in equilibrium, were separated and characterized by time-resolved emission spectroscopy on long time scales. The higher energy and faster emission process is assigned to the ^{3}MLCT state by quantitative comparison to the Re(phen)$(CO)_3$Cl model complex, whereas the lower energy, long lifetime component was assigned to the ^{3}LC state on the PNI subunit. The energy gap between the two triplet states in solution at RT was calculated to be 1680 cm^{-1} from the observed decay rate extrapolated to infinite dilution and eq 1, using the decay rate of the Re(I) model complex along with that of the long component determined for ^{3}LC in the frozen glass.

CONCLUSIONS

Attachment of the PNI chromophore to the MLCT core in **1** as a phen-based diimine ligand increased both the visible light harvesting capacity of the complex and rather impressively enhanced the excited state lifetime by 3000-fold with respect to the Re(phen)$(CO)_3$Cl parent structure, but retaining the same quantum yield. The dramatic increase in lifetime resulted

from the fairly large energy difference (1680 cm^{-1}) between the lower energy ^{3}LC state and the ^{3}MLCT state, strongly favoring the former in the equilibrium mixture and imparting "pure" PNI organic triplet-like photophysics into the ^{3}MLCT* decay. A powerful combination of transient absorption and infrared spectroscopy, each on the femtosecond and nanosecond time scales, combined with fluorescence decay kinetics enabled by TCSPC in concert with transient photoluminescence experiments facilitated the elucidation of all the intermediates involved in the evolution of the excited state decay processes exhibited by **1**. The only intermediate state not directly detected was inferred to be involved in excited state evolution by comparing Förster resonance energy transfer parameters to the observed ^{1}PNI* quenching rates, both found to be in excellent agreement. In instances where select assignments were not feasible by transient absorption spectroscopy, the corresponding transient infrared experiments enabled clear monitoring of that specific state. In most cases, the origin of select excited state intermediates could indeed be observed by multiple techniques, which simply aided in reinforcing the spectroscopic assignments and kinetic processes. The title chromophore represents an interesting example of bidirectional "ping-pong" energy transfer wherein photon excitation first migrates away from the initially prepared ^{1}PNI* excited state and then ultimately returns to this species as a long-lived excited triplet. Because the ^{3}PNI decays so it slowly disposes of its energy by equilibrating with a photoluminescent Re(I) MLCT excited state having a faster decay rate, resulting in the same quantum yield as the model $Re(phen)(CO)_3Cl$ complex but exhibiting a thermal average lifetime of 650 μs at RT.

EXPERIMENTAL SECTION

Reagents and Chemicals. All synthetic manipulations were performed under an inert and dry argon atmosphere using standard techniques. Piperidine, 4-nitronaphthalene-1,8-dicarboxyanhydride, 2,2,4-trimethylpentane, $Re(CO)_5Cl$, and *N*,*N*-dimethylformamide (DMF) were obtained from Sigma-Aldrich and used as received. 5-Amino-1,10-phenanthroline was purchased from Polysciences and used without further purification. *N*-(4-methylphenyl)-4-(1-piperidinyl)naphthalene-1,8-dicarboximide (PNI) was available from our previous study.[36] All other reagents were obtained from commercial sources and used as received.

***N*-(1,10-phenanthroline)-4-nitronaphthalene-1,8-dicarboximide.** NNI-phen was prepared using the procedure from Tyson and co-workers.[36] 4-Nitronaphthalene-1,8-dicarboxyanhydride (374 mg, 1.54 mmol) and 5-amino-1,10-phenanthroline (300 mg, 1.54 mmol) were refluxed in anhydrous ethanol (50 mL) for 2 days. Once cool, precipitation was promoted by adding a small portion of cold petroleum ether. The light tan solid was collected on a fine frit and rinsed with cold ethanol and followed by rinsing with cold petroleum ether. The product was obtained in 53% yield and used without further purification producing analytical data consistent with that observed previously.[36] ^{1}H NMR ($CDCl_3$), δ: 9.25 (m, 2H), 8.95 (d, 1H), 8.80 (t, 2H), 8.47 (d, 1H), 8.29 (dd, 1H), 7.97−8.12 (m, 2H), 7.88 (s, 1H), 7.70 (dd, 1H), 7.58 (dd, 1H). EI-MS: m/z 420 (M^+). ESI-HRMS Found: 421.0941 (MH^+), $C_{24}H_{13}N_4O_4$ requires 421.0937.

***N*-(1,10-Phenanthroline)-4-(1-piperidinyl)naphthalene-1,8-dicarboximide (PNI-phen).** PNI-phen was prepared using a modified procedure from Tyson and co-workers.[36] *N*-(1,10-Phenanthroline)-4-nitronaphthalene-1,8-dicarboximide (343 mg, 0.81 mmol) and piperidine (404 μL, 4.05 mmol) were refluxed in anhydrous DMF (9 mL) for 2 h. Once cool, the reaction mixture was poured into CH_2Cl_2 (100 mL) and washed twice with water, dried over $MgSO_4$, and rotary evaporated to a dark residue. The residue was dissolved into a minimal amount of dry CH_2Cl_2 and slowly dripped into cold petroleum ether. The yellow precipitate was collected on a fine glass frit and rinsed with cold petroleum ether. Column chromatography was used to purify the compound using deactivated silica gel and CH_2Cl_2/methanol 25:1 as the eluent. The mass and ^{1}H NMR ($CDCl_3$) analytical data are consistent with that previously published.[36] Because of overlap with solvent, d^6-acetone was found to be a more suitable NMR solvent for this compound: ^{1}H NMR ($CO(CD_3)_2$), δ: 9.19 (m, 2H), 8.62 (m, 2H), 8.51 (d, 2H), 8.40 (m, 1H), 8.13 (s, 1H), 7.90 (m, 1H), 7.67−7.84 (m, 2H), 7.44 (d, 1H), 3.36 (m, 4H), 1.96 (m, 4H), 1.77 (m, 2H). EI-MS: m/z 458 (M^+). ESI-HRMS Found: 459.1812 (MH^+), $C_{29}H_{23}N_4O_2$ requires 459.1821.

Tricarbonylchloro(*N*-(1,10-phenathroline)-4-(1-piperidinyl)-napthalene-1,8-dicarboximide)-rhenium [Re(PNI-phen)-$(CO)_3$Cl] (1). 1 was prepared using a modified procedure from Guarr and co-workers.[77] $Re(CO)_5Cl$ (190 mg, 0.53 mmol) and *N*-(1,10-phenanthroline)-4-(1-piperidinyl)napthalene-1,8-dicarboximide were refluxed in 2,2,4-trimethylpentane (isooctane) for 6 h. Once cool, the solid was collected over a fine frit and washed with cold petroleum ether. The title compound was obtained in 47% yield after flash column purification. ^{1}H NMR (DMSO), δ: 9.53 (dd, 2H), 9.02 (d, 2H), 8.55 (m, 3H), 8.46 (dd, 1H), 8.18 (dd, 1H), 8.02 (dd, 1H), 7.91 (dd, 1H), 7.42 (dd, 1H), 3.30 (m, 4H), 1.88 (m, 4H), 1.71 (m, 2H). ^{13}C NMR (d^6-DMSO), δ: 24.33, 26.19, 54.53, 115.46, 115.71, 123.51, 126.18, 126.44, 127.46, 127.50, 129.19, 129.33, 129.97, 130.85, 131.47, 131.83, 133.15, 133.64, 136.17, 140.21, 146.14, 146.66, 154.50, 154.86, 157.91, 164.19, 164.83, 198.03. ^{1}H-^{1}H COSY spectra are presented in the Supporting Information. MALDI-TOF MS: m/z 764.29 (M^+), 729.36 ($M - Cl$)$^+$. ESI-HRMS: Found $[M + CO_2H]^+$ 809.0789, $C_{33}H_{23}N_4O_7ClRe$ requires 809.08134. FT-IR ATR ($\nu_{C\equiv O}$: 2025, 1915, 1871 cm^{-1}; $\nu_{C=O}$: 1697, 1655 cm^{-1}).

General Techniques. ^{1}H, ^{13}C, and 2D COSY NMR spectra were recorded on a Bruker Avance III 500 MHz instrument operating at working frequencies of 500 and 125 MHz for ^{1}H and ^{13}C, respectively. MALDI-TOF mass spectra were measured by a Bruker Daltonics Omniflex Spectrometer using dithranol as the primary matrix. Optical absorption spectra were measured on a Cary 50 Bio UV−vis spectrophotometer from Varian. Steady-state luminescence spectra were obtained on a QM-4/2006SE fluorescence spectrometer from Photon Technologies Incorporated. Static FT-IR spectra were measured with a Jasco 4100 FT-IR. Solid samples were measured using the ATR accessory while solutions were measured using a standard CaF_2 FTIR cell.

Nanosecond Transient Absorption Spectroscopy. Nanosecond transient absorption spectra were collected on a Proteus spectrometer (Ultrafast Systems) equipped with a 150 W Xe-arc lamp (Newport), a Chromex monochromator (Bruker Optics) equipped with two diffraction gratings blazed for visible and near-IR dispersion, respectively, and Si or InGaAs photodiode detectors (DET 10A and DET 10C, Thorlabs) optically coupled to the exit slit of the monochromator. Excitation at 410 nm with a power of 2.0 mJ/pulse from a computer-controlled Nd:YAG laser/OPO system from Opotek (Vibrant LD 355 II) operating at 10 Hz was directed to the sample with an optical absorbance of 0.6 at the excitation wavelength. A flow cell with a path length of 1-cm was used to prevent sample photodegradation. The data consisting of a 256-shot average were analyzed by Origin 8.0 software.[78]

Ultrafast Transient Absorption Spectroscopy. The primary laser system for the ultrafast transient absorption measurement was described previously.[79] The 800 nm laser pulses were produced at a 1 kHz repetition rate by a mode-locked Ti:sapphire laser (Hurricane, Spectra-Physics). The pulse width was determined to be (fwhm) 110 fs using an autocorrelator (Positive Light). The output from a Hurricane was split into pump (85%) and probe (8%) beams. The pump beam (800 nm) was sent into second harmonic generator (Super Tripler,

CSK) to obtain a 400 nm excitation source. The energy of the pump beam was 3 μJ/pulse. The probe beam (800 nm) was delayed by a delay stage (MM 4000, Newport) and then focused into a CaF_2 crystal for white light continuum generation between 330 and 800 nm. An optical chopper was used to modulate the excitation beam at 100 Hz frequency and obtain the value of the transient absorption signal. The relative polarization between the pump and the probe beams was set at the magic angle (54.7°). The pump and probe beams were overlapped in the sample. The flow cell (Spectrocell Inc., 0.7 mL volume with 2 mm path length), pumped by a variable flow peristaltic lab pump (VWR), was used to prevent photodegradation of the sample. After passing through the flow cell, the continuum was coupled into an optical fiber and input into a CCD spectrograph (Ocean Optics, S2000). The data acquisition was achieved using in-house LabVIEW (National Instruments) software routines.[80] Alternatively, another pump−probe system was utilized that has been described in detail elsewhere.[81]

Nanosecond Step-Scan FTIR. TRIR experiments were performed using instrumentation based on a Bruker IFS-55 FT-IR spectrometer with 8 cm^{-1} resolution, placed on a laser table equipped with vibration isolation support. Excitation was performed at 410 nm with a power of 2.0 mJ/pulse from a computer-controlled Nd:YAG laser/OPO system from Opotek (Vibrant LD 355 II) operating at 10 Hz. Experiments were performed on the sample in argon-deaerated THF using two CaF_2 windows separated by a 330 μm spacer, configured as a flow cell (10 mL/min). The compound was probed from 2600 to 1400 cm^{-1}, and the data was averaged 64 times per time slice.[60a]

Ultrafast Time-Resolved Infrared Spectroscopy. Mid-IR transient absorption spectra were obtained using the femtosecond pump−probe setup described previously.[82] The source of femtosecond pulses at 800 nm (1 kHz repetition rate, ~90 fs pulse width) was a Ti:Sapphire oscillator/regenerative amplifier (Hurricane, Spectra Physics). The output from the amplifier was split into two beams, and the wavelengths for pump and probe beams were obtained using two TOPAS-C systems (Quantronix/Light Conversion). The pump pulses at 410 nm were chopped at 500 Hz frequency using an optical chopper (C-995, Terahertz Technologies Inc.) and time-delayed using a motorized translation stage (ILS 250 mm, Newport). The energy of the pump beam at the sample was about 2 μJ/pulse. Pump and probe beams were set at magic angle (54.7°) using a UV polarizer (ThorLabs) for the pump beam. The portion of the probe beam was split to produce reference and probe beams, and both beams were directed through a sample cell. The sample solution flow was achieved using a variable flow peristaltic lab pump (VWR) through a demountable liquid flow cell with Swagelok fittings (DSC-S25, Harrick Scientific Products Inc.). The path length was 250 μm, which was created by Teflon spacer between two round CaF_2 windows (25 × 2 mm, REFLEX Analytical Corporation). After passing through the sample cell, the probe and reference beams were directed to a Chromex Imaging Spectrograph (250 IS/SM), and the signal was read by a 2 × 32 array of MCT detectors (Infrared Systems Development Corporation). Before the transient IR measurement, the femtosecond TRIR system was purged by dry air for about 30 min to remove water and CO_2. The dry air was produced by a PCR compressed air dryer (PCR-SBX-1A-64FM, Puregas). The experimental data were collected using in-house LabView software (Version 7.1) and analyzed using Origin 8 software.

Time-Correlated Single Photon Counting (TCSPC). Time-resolved fluorescence experiments were accomplished using a time-correlated single photon counting (TCSPC) spectrometer (Edinburgh Instruments, LifeSpec II). Fluorescence signals were measured using a microchannel plate photomultiplier tube (Hamamatsu R3809U-50) in a Peltier-cooled housing. A Ti:Sapphire laser (Chameleon Ultra II, Coherent) was utilized as the excitation light source. Laser power was monitored using a Molectron Power Max 5200 power meter. For fluorescence intensity decay measurements, the Chameleon laser was tuned to 820 nm, pulse picked to a 4 MHz repetition rate (Coherent 9200 Pulse Picker), and finally frequency doubled (APE-GmbH SHG Unit) to afford sample excitation, λ_{ex} = 410 nm. The TCSPC fluorescence intensity decays were analyzed using Edinburgh FAST software.[83]

Time-Resolved Photoluminescence Intensity Decays. Single wavelength emission intensity decays of Re(PNI-phen)$(CO)_3$Cl and Re(phen)$(CO)_3$Cl at 77 K and room temperature were acquired with a N_2 pumped dye laser (2−3 nm fwhm) from PTI (GL-3300 N_2 laser, GL-301 dye laser) using an apparatus that has been previously described[34] with a few minor modifications. Excitation was achieved using POPOP as the dye with the wavelength tuned to 410 nm. Photoluminescence transients were collected at 650 nm for most experiments, with all exceptions noted in text. Time-resolved emission spectra of Re(PNI-phen)$(CO)_3$Cl was achieved by varying the emission monochromator wavelength while maintaining all other instrumental parameters constant.

■ ASSOCIATED CONTENT

Supporting Information. Additional static and time-resolved spectra, structural characterization data for Re(PNI-phen)$(CO)_3$Cl, and tabulated vibrational frequencies. This material is available free of charge via the Internet at http://pubs.acs.org.

■ AUTHOR INFORMATION

Corresponding Author

*Phone: (419) 372-7513. Fax: (419) 372-9809. E-mail castell@bgsu.edu.

■ ACKNOWLEDGMENT

The authors thank Prof. Ksenija D. Glusac for help with the ultrafast time-resolved IR measurements and Prof. Alexander N. Tarnovsky, Dr. Patrick Z. El-Khoury, and Dr. Fabian Spänig for their assistance with the ultrafast transient absorption measurements. This research was supported by the National Science Foundation (CHE-0719050 and CHE-1012487), the Air Force Office of Scientific Research (FA9550-05-1-0276), and the Ohio Research Scholars Program (J.C.D.).

■ REFERENCES

(1) Balzani, V., Campagna, S., Eds.; *Photochemistry and Photophysics of Coordination Compounds II*; Springer: New York, 2007.
(2) Vlček, A. *Top. Organomet. Chem.* **2010**, *29*, 73–114.
(3) O'Regan, B.; Graetzel, M. *Nature* **1991**, *353*, 737–740.
(4) *Photosensitization and Photocatalysis Using Inorganic and Organometallic Compounds*; Kalyanasundaram, K., Grätzel, M., Eds.; Kluwer: Dordrecht, The Netherlands, 1993.
(5) *Topics in Fluorescence Spectroscopy, Vol. 4: Probe Design and Chemical Sensing*; Lakowicz, J. R., Ed.; Plenum Press: New York, 1994.
(6) Szmacinski, H.; Lakowicz, J. R. *Sens. Actuators, B* **1995**, *29*, 16–24.
(7) de Silva, A. P.; Gunaratne, H. Q. N.; Gunnlaugsson, T.; Huxley, A. J. M.; McCoy, C. P.; Rademacher, J. T.; Rice, T. E. *Chem. Rev.* **1997**, *97*, 1515–1566.
(8) Beer, P. D. *Acc. Chem. Res.* **1998**, *31*, 71–80.
(9) Castellano, F. N.; Lakowicz, J. R. *Photochem. Photobiol.* **1998**, *67*, 179–183.
(10) Lakowicz, J. R.; Castellano, F. N.; Dattelbaum, J. D.; Tolosa, L.; Rao, G.; Gryczynski, I. *Anal. Chem.* **1998**, *70*, 5115–5121.
(11) Slone, R. V.; Benkstein, K. D.; Belanger, S.; Hupp, J. T.; Guzei, I. A.; Rheingold, A. L. *Coord. Chem. Rev.* **1998**, *171*, 221–243.
(12) Lakowicz, J. R. *Principles of Fluorescence Spectroscopy*, 2nd ed.; Kluwer Academic/Plenum Publishers: New York, 1999.
(13) Sun, S.-S.; Lees, A. J. *Chem. Commun.* **2000**, 1687–1688.

(14) Demas, J. N.; DeGraff, B. A. *Coord. Chem. Rev.* **2001**, *211*, 317–351.
(15) Terpetschnig, E.; Szmacinski, H.; Malak, H.; Lakowicz, J. R. *Biophys. J.* **1995**, *68*, 342–350.
(16) Guo, X.-Q.; Castellano, F. N.; Li, L.; Lakowicz, J. R. *Anal. Chem.* **1998**, *70*, 632–637.
(17) Balzani, V.; Scandola, F. *Supramolecular Photochemistry*; Horwood: Chichester, England, 1991.
(18) Lehn, J.-M. *Supramolecular Chemistry: Concepts and Prospectives*; VCH: Weinheim, Germany, 1995.
(19) Hayashi, Y.; Kita, S.; Brunschwig, B. S.; Fujita, E. *J. Am. Chem. Soc.* **2003**, *125*, 11976–11987.
(20) Takeda, H.; Koike, K.; Inoue, H.; Ishitani, O. *J. Am. Chem. Soc.* **2008**, *130*, 2023–2031.
(21) Probst, B.; Kolano, C.; Hamm, P.; Alberto, R. *Inorg. Chem.* **2009**, *48*, 1836–1843.
(22) Probst, B.; Rodenberg, A.; Guttentag, M.; Alberto, R. *Inorg. Chem.* **2010**, *49*, 6453–6460.
(23) Smieja, J. M.; Kubiak, C. P. *Inorg. Chem.* **2010**, *49*, 9283–9289.
(24) Juris, A.; Balzani, V.; Barigelletti, F.; Campagna, S.; Belser, P.; Von Zelewsky, A. *Coord. Chem. Rev.* **1988**, *84*, 85–277.
(25) Demas, J. N.; DeGraff, B. A. *Anal. Chem.* **1991**, *63*, 829A–837A.
(26) Kalyanasundaram, K. *Photochemistry of Polypyridine and Porphyrin Complexes*; Academic Press: San Diego, 1992.
(27) Shaw, J. R.; Schmehl, R. H. *J. Am. Chem. Soc.* **1991**, *113*, 389–394.
(28) Baba, A. I.; Shaw, J. R.; Simon, J. A.; Thummel, R. P.; Schmehl, R. H. *Coord. Chem. Rev.* **1998**, *171*, 43–59.
(29) Ford, W. E.; Rodgers, M. A. J. *J. Phys. Chem.* **1992**, *96*, 2917–2920.
(30) Simon, J. A.; Curry, S. L.; Schmehl, R. H.; Schatz, T. R.; Piotrowiak, P.; Jin, X.; Thummel, R. P. *J. Am. Chem. Soc.* **1997**, *119*, 11012–11022.
(31) Wilson, G. J.; Launikonis, A.; Sasse, W. H. F.; Mau, A. W. H. *J. Phys. Chem. A* **1997**, *101*, 4860–4866.
(32) Wilson, G. J.; Launikonis, A.; Sasse, W. H. F.; Mau, A. W. H. *J. Phys. Chem. A* **1998**, *102*, 5150–5156.
(33) Harriman, A.; Hissler, M.; Khatyr, A.; Ziessel, R. *Chem. Commun.* **1999**, 735–736.
(34) Tyson, D. S.; Castellano, F. N. *J. Phys. Chem. A* **1999**, *103*, 10955–10960.
(35) Tyson, D. S.; Bialecki, J.; Castellano, F. N. *Chem. Commun.* **2000**, 2355–2356.
(36) Tyson, D. S.; Luman, C. R.; Zhou, X.; Castellano, F. N. *Inorg. Chem.* **2001**, *40*, 4063–4071.
(37) Tyson, D. S.; Henbest, K. B.; Bialecki, J.; Castellano, F. N. *J. Phys. Chem. A* **2001**, *105*, 8154–8161.
(38) McClenaghan, N. D.; Barigelletti, F.; Maubert, B.; Campagna, S. *Chem. Commun.* **2002**, 602–603.
(39) Passalacqua, R.; Loiseau, F.; Campagna, S.; Fang, Y.-Q.; Hanan, G. S. *Angew. Chem., Int. Ed.* **2003**, *42*, 1608–1611.
(40) (a) Michalec, J. F.; Bejune, S. A.; McMillin, D. R. *Inorg. Chem.* **2000**, *39*, 2708–2709. (b) Montes, V. A.; Rodgers, M. A. J.; Anzenbacher, P., Jr. *Inorg. Chem.* **2007**, *46*, 10464–10466.
(41) Whited, M. T.; Djurovich, P. I.; Roberts, S. T.; Durrell, A. C.; Schlenker, C. W.; Bradforth, S. E.; Thompson, M. E. *J. Am. Chem. Soc.* **2011**, *133*, 88–96.
(42) El-ghayoury, A.; Harriman, A.; Ziessel, R. *Chem. Commun.* **1999**, 2027–2028.
(43) Laine, P. P.; Bedioui, F.; Loiseau, F.; Chiorboli, C.; Campagna, S. *J. Am. Chem. Soc.* **2006**, *128*, 7510–7521.
(44) Kalinowski, J.; Stampor, W.; Cocchi, M.; Virgili, D.; Fattori, V.; Di Marco, P. *Chem. Phys.* **2004**, *297*, 39–48.
(45) Leydet, Y.; Bassani, D. M.; Jonusauskas, G.; McClenaghan, N. D. *J. Am. Chem. Soc.* **2007**, *129*, 8688–8689.
(46) Deaton, J. C.; Switalski, S. C.; Kondakov, D. Y.; Young, R. H.; Pawlik, T. D.; Giesen, D. J.; Harkins, S. B.; Miller, A. J. M.; Mickenberg, S. F.; Peters, J. C. *J. Am. Chem. Soc.* **2010**, *132*, 9499–9508.
(47) Cohen, B. W.; Lovaasen, B. M.; Simpson, C. K.; Cummings, S. C.; Dallinger, R. F.; Hopkins, M. D. *Inorg. Chem.* **2010**, *49*, 5777–5779.
(48) Lavie-Cambot, A.; Lincheneau, C.; Cantuel, M.; Leydet, Y.; McClenaghan, N. D. *Chem. Soc. Rev.* **2010**, *39*, 506–515.
(49) Caspar, J. V.; Meyer, T. J. *J. Phys. Chem.* **1983**, *87*, 952–957.
(50) Kober, E. M.; Caspar, J. V.; Lumpkin, R. S.; Meyer, T. J. *J. Phys. Chem.* **1986**, *90*, 3722–3734.
(51) Strouse, G. F.; Schoonover, J. R.; Duesing, R.; Boyde, S.; Jones, W. E., Jr.; Meyer, T. J. *Inorg. Chem.* **1995**, *34*, 473–487.
(52) Damrauer, N. H.; Boussie, T. R.; Devenney, M.; McCusker, J. K. *J. Am. Chem. Soc.* **1997**, *119*, 8253–8268.
(53) Abrahamsson, M.; Jäger, M.; Kumar, R. J.; Österman, T.; Persson, P.; H.-C., B.; Hammarström, L. *J. Am. Chem. Soc.* **2008**, *130*, 15533–15542.
(54) *Highly Efficient OLEDs with Phosphorescent Materials*; Yersin, H., Ed.; Wiley-VCH Verlag GmbH & Co., KgaA: Weinheim, Germany, 2008.
(55) Wu, C.; Djurovich, P. I.; Roberts, S. T.; Durrell, A. C.; Schlenker, C. W.; Bradforth, S. E.; Thompson, M. E. *Adv. Funct. Mater.* **2009**, *19*, 3157–3164.
(56) Kondakova, M. E.; Deaton, J. C.; Pawlik, T. D.; Giesen, D. J.; Kondakov, D. Y.; Young, R. H.; Royster, T. L.; Comfort, D. L.; Shore, J. D. *J. Appl. Phys.* **2010**, *107*, 014515.
(57) Guo, F.; Ogawa, K.; Kim, Y.-G.; Danilov, E. O.; Castellano, F. N.; Reynolds, J. R.; Schanze, K. S. *Phys. Chem. Chem. Phys.* **2007**, *9*, 2724–2734.
(58) Singh-Rachford, T. N.; Castellano, F. N. *Coord. Chem. Rev.* **2010**, *254*, 2560–2573.
(59) Walters, K. A.; Ley, K. D.; Cavalaheiro, C. S. P.; Miller, S. E.; Gosztola, D.; Wasielewski, M. R.; Bussandri, A. P.; Van Willigen, H.; Schanze, K. S. *J. Am. Chem. Soc.* **2001**, *123*, 8329–8342.
(60) (a) Polyansky, D. E.; Danilov, E. O.; Castellano, F. N. *Inorg. Chem.* **2006**, *45*, 2370–2372. (b) Sazanovich, I. V.; Alamiry, M. A. H.; Best, J.; Bennett, R. D.; Bouganov, O. V.; Davies, E. S.; Grivin, V. P.; Meijer, A. J. H. M.; Plyusnin, V. F.; Ronayne, K. L.; Shelton, A. H.; Tikhomirov, S. A.; Towrie, M.; Weinstein, J. A. *Inorg. Chem.* **2008**, *47*, 10432–10445.
(61) Wrighton, M.; Morse, D. L. *J. Am. Chem. Soc.* **1974**, *96*, 998–1003.
(62) Middleton, R. W.; Parrick, J.; Clarke, E. D.; Wardman, P. *J. Heterocycl. Chem.* **1986**, *23*, 849–855.
(63) Alexiou, M. S.; Tychopoulos, V.; Ghorbanian, S.; Tyman, J. H. P.; Brown, R. G.; Brittain, P. I. *J. Chem. Soc., Perkin Trans. 2* **1990**, 837–842.
(64) de Silva, A. P.; Qunaratne, H. Q. N.; Habib-Jiwan, J.-L.; McCoy, C. P.; Rice, T. E.; Soumillion, J.-P. *Angew. Chem., Int. Ed. Engl.* **1995**, *34*, 1728–1731.
(65) Greenfield, S. R.; Svec, W. A.; Gosztola, D.; Wasielewski, M. R. *J. Am. Chem. Soc.* **1996**, *118*, 6767–6777.
(66) Forster, T. *Ann. Physik* **1948**, *2*, 55–75.
(67) Forster, T. *Z. Naturforsch.* **1949**, *4a*, 321–327.
(68) Dixon, J. M.; Taniguchi, M.; Lindsey, J. S. *Photochem. Photobiol.* **2005**, *81*, 212–213.
(69) Tyson, D. S.; Bialecki, J.; Castellano, F. N. *Chem. Commun.* **2000**, 2355–2356.
(70) Pomestchenko, I. E.; Polyansky, D. E.; Castellano, F. N. *Inorg. Chem.* **2005**, *44*, 3412–3421.
(71) Barboy, N.; Feitelson, J. *Anal. Biochem.* **1989**, *180*, 384–386.
(72) Rossenaar, B. D.; Stufkens, D. J.; Vlček, A. *Inorg. Chem.* **1996**, *35*, 2902–2909.
(73) El Nahhas, A.; Cannizzo, A.; van Mourik, F.; Blanco-Rodriguez, A. M.; Zalis, S.; Vlček, A.; Chergui, M. *J. Phys. Chem. A* **2010**, *114*, 6361–6369.
(74) Cannizzo, A.; Blanco-Rodriguez, A. M.; El Nahhas, A.; Sebera, J.; Zalis, S.; Vlcek, A., Jr.; Chergui, M. *J. Am. Chem. Soc.* **2008**, *130*, 8967–8974.
(75) George, M. W.; Johnson, F. P. A.; Westwell, J. R.; Hodges, P. M.; Turner, J. J. *J. Chem. Soc., Dalton Trans.* **1993**, 2977–2979.

(76) Schoonover, J. R.; Strouse, G. F.; Dyer, R. B.; Bates, W. D.; Chen, P.; Meyer, T. J. *Inorg. Chem.* **1996**, *35*, 273–274.
(77) Lin, R.; Fu, Y.; Brock, C. P.; Guarr, T. F. *Inorg. Chem.* **1992**, *31*, 4346–4353.
(78) Danilov, E. O.; Rachford, A. A.; Goeb, S.; Castellano, F. N. *J. Phys. Chem. A* **2009**, *113*, 5763–5768.
(79) Nikolaitchik, A. V.; Korth, O.; Rodgers, M. A. J. *J. Phys. Chem. A* **1999**, *103*, 7587–7596.
(80) Li, G. F.; Glusac, K. D. *J. Phys. Chem. A* **2008**, *112*, 4573–4583.
(81) El-Khoury, P. Z.; Tarnovsky, A. N. *Chem. Phys. Lett.* **2008**, *453*, 160–166.
(82) Li, G. F.; Sichula, V.; Glusac, K. D. *J. Phys. Chem. B* **2008**, *112*, 10758–10764.
(83) Singh-Rachford, T. N.; Castellano, F. N. *J. Phys. Chem. A* **2009**, *113*, 9266–9269.